Nanostructured Optical Photonic Crystal Biosensor for HIV Viral Load Measurement

Hadi Shafiee[1], Erich A. Lidstone[2], Muntasir Jahangir[1], Fatih Inci[1], Emily Hanhauser[3], Timothy J. Henrich[3], Daniel R. Kuritzkes[3], Brian T. Cunningham[2] & Utkan Demirci[1,3,4]

[1]Bio-Acoustic MEMS in Medicine (BAMM) Laboratory, Division of Biomedical Engineering, Department of Medicine, Brigham and Women's Hospital, Harvard Medical School, Boston, MA, USA, [2]Department of Electrical & Computer Engineering, and Department of Bioengineering, University of Illinois at Urbana-Champaign, IL, USA, [3]Division of Infectious Diseases, Brigham and Women's Hospital, Harvard Medical School, MA, USA, [4]Harvard-MIT Division of Health Sciences and Technology, Cambridge, MA, USA.

Detecting and quantifying biomarkers and viruses in biological samples have broad applications in early disease diagnosis and treatment monitoring. We have demonstrated a label-free optical sensing mechanism using nanostructured photonic crystals (PC) to capture and quantify intact viruses (HIV-1) from biologically relevant samples. The nanostructured surface of the PC biosensor resonantly reflects a narrow wavelength band during illumination with a broadband light source. Surface-adsorbed biotarget induces a shift in the resonant Peak Wavelength Value (PWV) that is detectable with <10 pm wavelength resolution, enabling detection of both biomolecular layers and small number of viruses that sparsely populate the transducer surface. We have successfully captured and detected HIV-1 in serum and phosphate buffered saline (PBS) samples with viral loads ranging from 10^4 to 10^8 copies/mL. The surface density of immobilized biomolecular layers used in the sensor functionalization process, including 3-mercaptopropyltrimethoxysilane (3-MPS), N-gamma-Maleimidobutyryl-oxysuccinimide ester (GMBS), NeutrAvidin, anti-gp120, and bovine serum albumin (BSA) were also quantified by the PC biosensor.

R apid and sensitive detection of proteins, antibodies, and pathogens in biological samples has broad applications in the prognosis and treatment monitoring of several diseases including immune response for infectious diseases, cancer, and cardiovascular disease[1,2,23,71]. For instance, cancer biomarker and cancer cells detection have shown great promise in early detection of colon, lung, ovarian, prostate, and leukemia cancers[3–13]. Further, rapid and sensitive detection of pathogens and infectious agents at the point-of-care (POC) is essential for disease diagnosis, microbial forensics[14], and public health[15]. More specifically, detecting human immunodeficiency virus (HIV) in biological samples is critical for HIV detection and treatment monitoring in resource-constrained settings[16–18]. The integration of nanotechnology and label-free optical, electrical, and mechanical biosensing has opened promising avenues in the development of diagnostic tools for infectious diseases and cancer[19–22,24,25].

Antiretroviral therapy (ART) has been a successful method utilized in suppressing acquired immunodeficiency syndrome (AIDS). However, a significant ratio of the AIDS patients in developing world do not receive ARTs due to limited availability of rapid, sensitive, inexpensive, and portable HIV diagnostic tools for viral load measurement and CD4 cell counting as the indicators of the patient's immune response to ART. For instance, 46% of the patients who needed ART worldwide by the end of 2011 did not receive therapy[26,27]. Flow cytometry and reverse transcription quantitative polymerase chain reaction (RT-qPCR) are sensitive standard methods for CD4 cell count and viral load measurements to monitor ART, but they require complex laboratory infrastructure, expensive reagents, and skilled operators[15,28]. Viral load measurement at the POC has been technically challenging and no POC viral load platform has been available commercially. Several POC CD4 cell count devices have been developed based upon World Health Organization (WHO) guidelines that recommend therapy initiation in resource-constrained settings when CD4 cell count falls below 500 cells/μL[29]. CD4 cell count alone, however, may lead to reducing the drug efficacy because early virological failure cannot be detected through this strategy[30–33]. Therefore, emerging new technologies are clinically needed to develop POC viral load measurement tools suitable for resource-constrained settings.
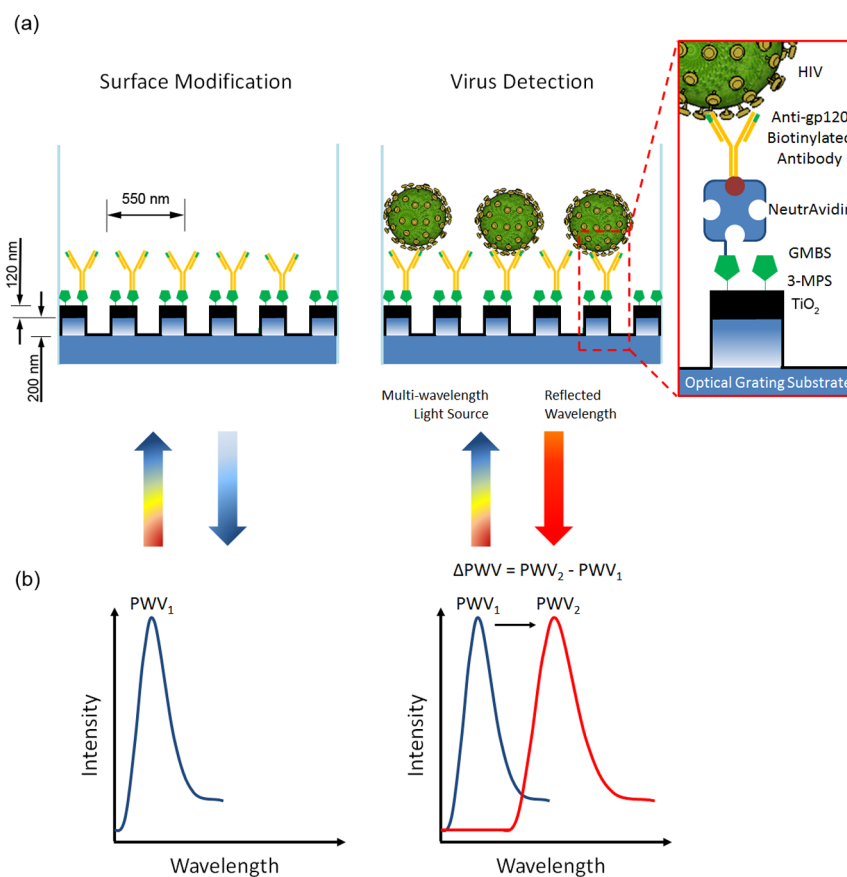
Figure 1 | Schematic of Photonic Crystal (PC) -based intact virus detection platform. (a) The bottom surface of PC biosensor microplate wells is comprised of a nanostructured subwavelength grating that is coated with TiO_2. (b) Binding events within the close vicinity of the sensing area change the bulk index of refraction, thus, the peak wavelength value (PWV) of the reflected light is altered. The shift in the peak wavelength (ΔPWV) is directly proportional to the binding of molecules and/or bioagents (*e.g.*, cells and viruses) onto the biosensing surface.

Several technologies have been developed for virus detection utilizing optical, electrical, and acoustic sensing methods such as surface plasmon resonance (SPR), localized surface plasmon resonance (LSPR), quartz crystal microbalance (QCM), nanowires, and impedance analysis[17,18,34–39]. A nanoplasmonic-based platform was developed to detect intact HIV-1 using self-assembled gold nanoparticles conjugated with biotinylated anti-gp120 polyclonal antibodies to selectively capture and detect HIV[18]. An electrical sensing mechanism was also developed to detect captured HIV-1 on magnetic beads conjugated with anti-gp120 antibodies through impedance spectroscopy of viral lysate samples[17].

Among these approaches, photonic crystal (PC) biosensors offer a rapid and sensitive optical detection method for biomolecules, cells, and viruses by monitoring the dielectric permittivity changes at the interface of a transducer substrate and a liquid media[40]. Periodic arrangement of dielectric material on a PC sensor results in establishment of an optical resonance at a precise wavelength, at which electromagnetic standing waves form, which extend into the liquid media in contact with the PC surface (Figure 1). The PC nanostructures are comprised of a periodic surface structure formed by replica molding from a low refractive index polymer, which is coated with a high refractive index TiO_2 dielectric layer. When illuminated with a collimated broadband light source at normal incidence, the PC structure reflects only a narrow resonant band of wavelengths with nearly 100% efficiency, while all other wavelengths pass through. The Peak Wavelength Value (PWV) of the reflected resonant spectrum shifts to greater values when biological analytes, such as proteins, viruses, or cells bind to the PC. For instance, PC surfaces were used to detect breast cancer cell (MCF-7) cytotoxicity and proliferation[41] and

porcine rotavirus in biological samples[38]. PC biosensors have also been used in high throughput analysis of kinetic biomolecular interactions[42]. Here, we have developed a PC biosensing platform that captures and detects intact viruses (HIV-1) as well as biomolecules and antibodies. Multiple HIV-1 subtypes (A, B, and D) were detected in spiked samples with viral loads ranging from 10^4 to 10^8 copies/mL and validated with the gold standard method (*i.e.*, RT-qPCR).

Results

To evaluate surface activation and biomolecule binding events, a control group of unmodified PC surfaces were used. After modification with the surface activators (*i.e.*, 3-mercaptopropyltrimethoxysilane (3-MPS) and N-gamma-Maleimidobutyryl-oxysuccinimide ester (GMBS)), PWV shift of 0.35 ± 0.15 nm was measured (Figure 2). The corresponding PWV shifts were analyzed using Analysis of Variance (ANOVA) statistical analysis represented a statistically significant difference from the unmodified PC surface ($n = 3$, $p < 0.05$) (Figure 2). GMBS molecules presented succinimide groups to bind NeutrAvidin, which allowed antibody immobilization with a favorable orientation for a higher capture efficiency rather than physical adsorption and chemical binding[16]. After modification of PC surfaces with NeutrAvidin, the PWV shift was measured to be 1.24 ± 0.10 nm (Figure 2). Statistical analysis was performed for NeutrAvidin step, and demonstrated that there was a statistically significant difference compared to the previous step ($n = 3$, $p < 0.05$) (Figure 2). The immobilization of biotinylated anti-gp120 polyclonal antibodies on PC surfaces caused a PWV shift of 1.90 ± 0.13 nm, which was statistically different compared to NeutrAvidin step ($n = 3$, $p < 0.05$) (Figure 2). 10% BSA was used as a blocking agent to
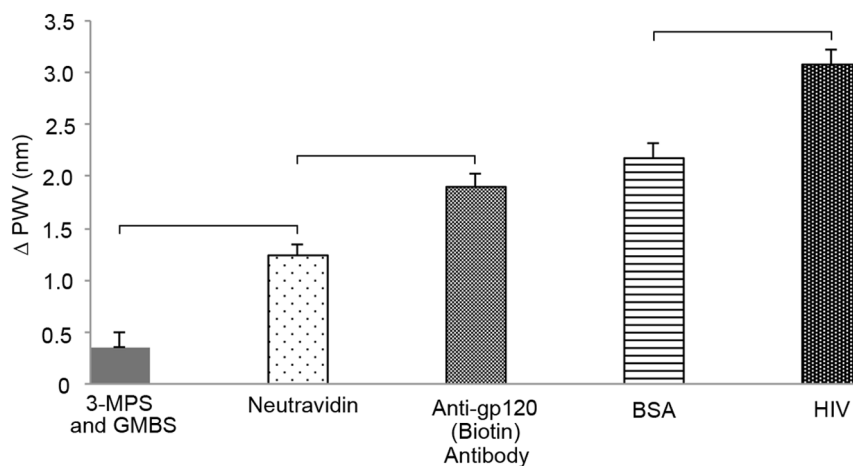
Figure 2 | PWV Shift due to Surface Chemistry. Utilizing a 384-well plate, each step of the surface chemistry process produced a distinct wavelength shift after incubation. The plate was initially washed 3× with DPBS, treated with plasma for 2 minutes, then incubated with 3-MPS at room temperature for 30 minutes, followed by GMBS incubation for 30 minutes at room temperature. Next, NeutrAvidin and anti-gp120 antibody were added sequentially, each with 1 hour incubation at +4°C. Blocking was performed using BSA for 30 minutes at +4°C. Viruses (subtype D, 2.9×10^8 copies/mL) were incubated for 30 minutes at room temperature, fixed with 4% paraformaldehyde, and washed again with DPBS. ΔPWV is based off of shift from DPBS baseline step, which was set to zero. Statistical assessment on the results was performed using Analysis of Variance (ANOVA) with Tukey posthoc test for multiple comparisons. Statistical significance threshold was set at 0.05, $p < 0.05$. Error bars represent standard error of the mean ($n = 3$). Brackets connecting individual groups indicate statistically significant PWV shift.

prevent nonspecific binding on PC surface and this step did not cause a statistically significant peak shift compared to the antibody step ($n = 3$, $p > 0.05$) (Figure 2). The PWV shift after blocking the PC surface with BSA was 2.18 ± 0.14 nm.

To further evaluate the ability of the PC platform for virus (HIV-1) capture and detection. We tested HIV-1 spiked in DPBS samples at concentrations ranging from 10^4 to 10^8 copies/mL (Figure 3). The PWV shifts for the virus samples were measured with respect to PWV corresponding to PC surfaces conjugated with antibodies before the virus capture step. The PWV shifts for HIV-1 subtype B and D spiked in DPBS samples represented a statistically significant difference compared to control samples at minimum viral loads of 10^6 copies/mL and 10^5 copies/mL, respectively (Figures 3 a,b, $n = 3$, $p < 0.05$). There was no significant PWV shift observed for viral loads below 10^5 copies/mL (Figures 3 a,b, $n = 3$, $p > 0.05$). Linear curve fits that correlate viral loads in HIV-spiked in DPBS samples to the corresponding PWV shifts were calculated for HIV-1 subtypes B and D (Figures S1a, b). The coefficients of determination (R^2) for these linear curve fits were 0.92 and 0.96 for subtypes B and D, respectively. We have also evaluated the repeatability of the PWV shift measurements for samples with virus concentrations ranging from 10^5 to 10^8 copies/mL for HIV-1 subtypes B and D. The repeatability was calculated based on the following equation:

$$Repeatability = \frac{PWV\ change\ mean}{PWV\ change\ mean + standard\ error\ of\ measurement} \times 100$$

The repeatability of the experimental measurements for PWV shifts for HIV-1 subtype B using samples with viral loads of 10^5, 10^6, 10^7, and 10^8 copies/mL were 85%, 85%, 89%, and 91%, respectively ($n = 3$) (Figure 3c) and for HIV-1 subtype D were 85%, 93%, 95%, and 98%, respectively ($n = 3$) (Figure 3d). We have also used scanning electron microscopy (SEM) to visualize captured HIV-1 on the surface of the PC substrates (Figure 4).

Excessive levels of protein including albumin, casein, and immunoglobin due to presence of HIV-1 in biological samples may prevent antigen/antibody interactions and create nonspecific binding[16]. It has been shown that anti-gp120 antibody is highly specific in capturing multiple HIV-1 subtypes in whole blood and HIV-infected patient samples[16,18] as well as in the presence of other viruses such as

Epstein-Bar Virus (EBV)[17]. To evaluate the specificity of the PC-based platform and potential drift due to nonspecific binding on the nanostructured surfaces, we tested the biosensing system with HIV-spiked plasma samples with various viral loads between 10^2 and 10^7 copies/mL. Plasma without HIV-1 was used as a control sample. The viral loads of the stock HIV-1 samples were quantified by RT-qPCR as the gold standard method. The PWV shift of the spiked plasma samples with HIV-1 subtype B with viral loads of 10^2, 10^3, and 10^4 copies/mL were not significantly different compared to control samples (Figure S2a, $n = 3$, $p > 0.05$). The PWV shifts of the spiked plasma samples with HIV-1 subtype B with viral loads of 10^5, 10^6, and 10^7 copies/mL were significantly higher than the PWV shift of the control samples (Figure S2a, $n = 3$, $p < 0.05$). We also observed that the PWV shift of the spiked plasma samples with viral load of 10^5 copies/mL was significantly different than all other spiked plasma samples (Figure S2a, $n = 3$, $p < 0.05$). The PWV shifts of plasma samples spiked with HIV-1 subtype B were 2.82 ± 0.11 nm (control), 2.97 ± 0.10 nm (10^2 copies/mL), 3.14 ± 0.13 nm (10^3 copies/mL), 3.61 ± 0.60 nm (10^4 copies/mL), 5.03 ± 0.30 nm (10^5 copies/mL), 3.77 ± 0.32 nm (10^6 copies/mL), and 4.10 ± 0.16 nm (10^7 copies/mL). The linear correlation between the PWV shifts of the HIV-spiked plasma samples with viral loads between 10^2 and 10^7 copies/mL was also calculated as illustrated in Figure S2b. The repeatability of these PWV shift measurements was between 91% and 98% for HIV-1 subtype B (Figure S2c). Thus, the PC substrates functionalized with anti-gp120 antibodies selectively and reproducibly captured HIV-1 in plasma. The PWV shift decreased for spiked plasma samples with viral loads higher than 10^5 copies/mL. We observed the same response in plasma samples spiked with another subtype (subtype A) (Figure S3). Previously, negative PWV shifts were also reported for detection of porcine rotavirus on the photonic crystal surfaces[43]. The PWV shift is strongly dependent on the dimension of the 3D structures on the photonic crystal substrates including the height of the titanium oxide layer, the width of the slabs and the gap between the slabs. Proteins in serum samples can accumulate on the surface of the PC substrates due to nonspecific binding and change the dimensions of the PC slabs, which causes larger PWV shifts in spiked plasma samples compared to spiked DPBS samples. At higher virus concentrations, there seems to be a higher chance that free viruses in solution remove or extract accumulated proteins,
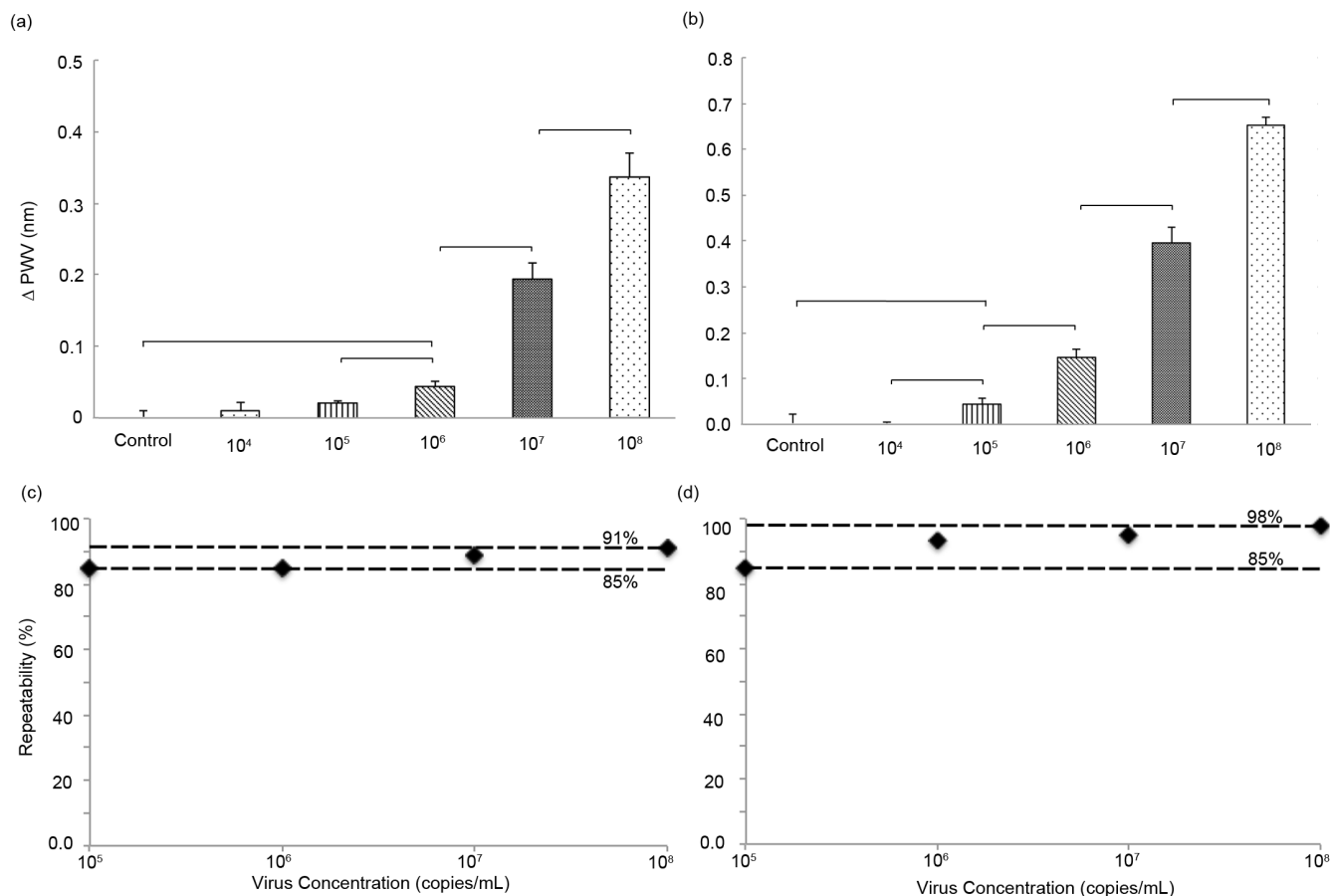
Figure 3 | Capturing and detecting HIV-1 on PC surfaces with corresponding PWV shift using two blocking methods. (a) BSA blocking using HIV-1 subtype B (b) Glycine blocking with HIV-1 subtype D. Utilizing the 384-well plate, normal surface chemistry was performed. ΔPWV is based upon the shift from the previous step of antibody incubation. All values have been referenced against a negative control without viruses. Repeatability measurement (n = 3) for spiked DPBS samples with virus concentrations ranging from 10^5 to 10^8 copies/mL for HIV-1 subtypes B (c) and D. (d) The repeatability of the experiments was between 85% and 91% for HIV-1 subtype B and between 85% and 98% for HIV-1 subtype D. Statistical assessment of the results was performed using unpaired t test with 95% confidence internal for multiple comparisons. Statistical significance threshold was set at 0.05. Error bars represent standard error of the mean (n = 3). Brackets connecting individual groups indicate statistically significant PWV shift (p < 0.05).

blocking agent, or antibodies from the PC surface[43]. Therefore, a drop in PWV shift is observed in spiked plasma samples with viral loads greater than 10^5 copies/mL. The high viral load measurements (*e.g.* >10^5 copies/mL) in spiked plasma samples would potentially benefit from further surface chemistry and design optimization on the photonic crystals.

Discussion

HIV/AIDS is a global pandemic that has caused 25 million deaths and more than 30 million people are infected worldwide[44–46]. The viral replication and shedding reaches its maximum rate at the acute HIV stage (10^6–10^8 copies/mL) and makes the acute HIV infection cases highly contagious[47–49]. Patients with acute HIV-1 infection,
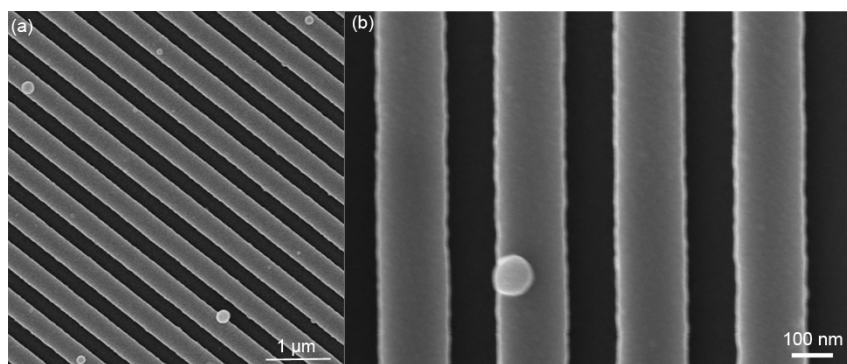

Figure 4 | Visualization of the captured viruses on photonic crystal surfaces. (a) Scanning Electron Microscopy (SEM) imaging of photonic crystal surfaces with captured HIV-1 (b) Close-up image of a single virus attached to the PC surface. Utilizing the 384-well plate, surface chemistry was performed using anti-gp120 antibody (20 µg/mL) and BSA blocking. Sample wells were washed with DPBS to remove unattached viruses, fixed with 4% paraformaldehyde, and further washed with HyClone® Grade Water followed by overnight drying through evaporation. SEM image was taken at 3.5 mm working distance and 5 kV accelerating voltage.

4

who are unaware of their disease, thus contribute substantially to HIV-1 transmission[50,51]. Current POC rapid HIV tests target antibodies against HIV-1 generated after infection. Recent comprehensive investigations on samples taken from patients at high risk of HIV infection and a field evaluation at Malawi have revealed that the available POC HIV tests have poor sensitivity in detecting acute HIV[52–54]. For instance, Determine™ HIV-1/2 Ag/Ab Combo rapid test (Combo RT) was not sensitive to detect HIV-1 subtypes F, G, H, J, CRF06_cpx, and CRF11_cpx and HIV-1 groups O and P and HIV-2. The sensitivity of this rapid test was 61.5% for subtype B[52,53]. Therefore, there is an unmet clinical need to detect HIV-1 at acute stage, where current antibody-based POC technologies such as lateral flow assays, including dipsticks, enzyme-linked immunosorbent assays (ELISA), and OraQuick are not effective due to the low concentration of antibodies[49,52,55].

Further, to increase access to ART, and to improve treatment outcomes, there is an urgent need for inexpensive diagnostic and monitoring tools[15,56,57]. In developed countries, HIV-1 viral load nucleic acid assays are used to monitor the treatment efficacy, to ensure patient adherence and to predict disease progression. Since HIV-1 viral load assays are expensive ($50–200 per test), instrument-dependent, and technically complex, CD4 cell count and clinical symptoms are used to guide ART in developing countries. Recent studies, however, have shown this strategy cannot detect early virological failure[30–32]. The virological failure causes accumulation of drug-resistance strains and reduces efficacy of the available second-line regimens in resource-constrained settings[32]. Thus, to increase access to ART, a rapid, inexpensive, and simple viral load test is urgently needed at the POC settings.

In this work, we have developed and presented an optical-based PC biosensing platform that can capture and detect HIV-1 in samples with clinically relevant viral loads ranging from 10^4 to 10^8 copies/mL that occur before the seroconversion stage of the HIV-1 infection (acute HIV-1)[48]. Previous published work demonstrated that multiple HIV-1 subtypes (A, B, C, D, E, G, and panel) were captured, isolated, and quantified using biotinylated goat anti-HIV gp120 polyclonal antibody, which targets multiple epitopes of gp120 on HIV-1 surface[16–18]. Although HIV-1 gp120 envelope sequences vary between HIV-1 subtypes, the antibody used in this work to capture HIV-1 (biotinylated goat anti-gp120, ab53937) is polyclonal, and therefore, targets multiple epitopes. In this paper, gp120 sequences for subtypes B and D were also aligned with the EU541617 reference strain used to generate the polyclonal antibody (Figures S4–S6).

Although anti-gp120 antibody used in this work is a polyclonal antibody, the sensitivity of the PC biosensor is related to the HIV-1 subtype. The different sensitivity and repeatability in these results are attributed to the differences between the HIV-1 gp120 envelope sequences of different subtypes (A, B and D) used in this work. Further, different subtypes can be captured and detected with different capture efficiencies and sensitivities[16,18]. Overall, anti-gp120 antibody captures different HIV-1 subtypes. Subtype specific antibodies could improve the overall capture efficiency and sensitivity per subtype.

It has been shown previously that rapid viral load replication and doubling time (10 hours) during the acute HIV infection and before ART initiation results in very high viral load levels (10^5–10^8 copies/mL)[47,48,58]. Although the maximum viral load is observed in acute HIV-infected patients varies, these studies showed that it can reach to a minimum of 10^5 copies/mL during the early stage of HIV-1 infection (seroconversion)[47]. Therefore, the PC-based assay developed and presented in this work can potentially be used to detect HIV in infected individuals before the seroconversion stage of infection.

Currently an assay with higher sensitivity to detect and quantify HIV in biological samples based on World Health Organization (WHO) definition of treatment failure (VL > 1,000 copies/mL)[59]

as well as the Department of Health and Human Services (DHHS) and AIDS Clinical Trials Group (ACTG) definitions of treatment failure (VL > 200 copies/mL)[60–62] would be beneficial to cover a larger population of the HIV-infected patients for HIV detection and ART monitoring. We envision that the sensitivity of this PC-based assay can be potentially further enhanced by integrating a microfluidic system that increases the capture efficiency of viruses by decreasing the distance between the target viruses in the sample and the PC surface[63–66]. In the current approach, samples are placed in microwells and viruses are captured at the bottom of the wells, which requires the viruses to diffuse for a relatively long distance to reach the capture zone on the surface of a PC substrate. A microfluidic channel would reduce the time required for diffusion to bring analyte to the sensing surface, and minimize the non-sensing surface area that is capable of adsorbing viral particles. Reduction of the antibody-prepared sensing area within a microfluidic channel will potentially result in an increase in virus surface density for a fixed virus concentration in the test sample, resulting in greater PWV shifts. Increasing antibody concentration and using other capture antibodies and moieties such as anti-gp41, anti-gp24 antibodies, soluble CD4 molecules, or a cocktail of these antibodies may also improve the capture efficiency and sensitivity of the assay. The selectivity and efficiency of these antibodies to capture HIV-1, needs to be further evaluated using the PC-based biosensor platform.

Although this PC-based sensing platform has shown a great promise in detecting HIV-1 at the early stage of HIV-infection (seroconversion) with high repeatability and selectivity, it needs further work towards a portable design. This assay requires only a fingerprick unprocessed whole blood sample (<50 μL) for HIV-1 detection and for a closed system with automated sample handling a biosafety level (BSL)2 or BSL2+ facility and virus culture are not needed.

Methods

Reagents. Dulbecco's Phosphate Buffered Saline (DPBS) was purchased from Life Technologies (Grand Island, NY). Reagents used for surface chemistry including 3-mercaptopropyltrimethoxysilane (3-MPS), N-gamma-Maleimidobutyryl-oxysuccinimide ester (GMBS), 200 proof of ethanol (EtOH), and paraformaldehyde were obtained from Sigma Aldrich (Sheboygan, WI). Proteins utilized in the surface chemistry including Bovine Serum Albumin (BSA) and NeutrAvidin were purchased from Fisher Scientific (Agawam, MA). The capture antibody, biotinylated anti-gp120 polyclonal antibody (ab53937), was purchased from Abcam® (Cambridge, MA).

PC well plate fabrication. PC biosensors were integrated with standard-format 384-well microplates, as described in previous work[67]. The PC is comprised of a flexible polyester substrate that is coated with a uniform, large-area grating structure (period = 550 nm, depth = 120 nm) that is overcoated by a titanium dioxide (TiO$_2$) thin film to produce a high efficiency resonant optical reflection at a wavelength of 855 nm. PC-based micro-well plates (SRU Biosystems 384 micro-well plates, 110421-0108-3MC, SRU Biosystems, Woburn, MA) are manufactured using a photoreplica-molding process that begins with a silicon master wafer into which ultraviolet light-curable polymer is molded, covered with a sheet of polyethylene, and cured using UV light. The polymer grating structure has a period of 550 nm and a grating depth of 200 nm. After the polymer sensor is cured and removed from the silicon master, fabrication is completed with the addition of a 120 nm-thick layer of TiO$_2$, which has a high refractive dielectric index, using a roll-to-roll reactive sputter deposition process. Sensor coupons are cut from the roll, and attached with adhesive to bottomless 384 micro-well plates, such that the entire bottom surface of each well is covered with the PC structure.

Layer-by-layer biomolecule and antibody immobilization. Prior to applying proteins and antibodies to the surface of the biosensor, a 384-well biosensor microplate was washed three times using 1× DPBS. After the final wash, DPBS was incubated in the wells and a PWV baseline was recorded for each well using a detection instrument specifically configured for rapidly scanning PC biosensor microplates (BIND Reader, SRU Biosystems, Woburn, MA). PWV shift for every microplate well was measured after each surface modification step. Briefly, 3-MPS (42.3 mg/mL in EtOH) was dispensed into the wells, and the plate was incubated at room temperature for 30 minutes. The wells were washed three times with 70% EtOH, and then, GMBS (0.28 mg/mL in EtOH) was added to the wells and incubated for 30 minutes. The plate was washed three times with DPBS to remove unbound and weakly bound non-adsorbed material. To immobilize antibodies, NeutrAvidin (0.10 mg/mL in DPBS) was incubated for an hour at room temperature. The plate was then washed three times with DPBS, and then, incubated with a blocking agent, 10% BSA in DPBS, for 30 minutes at room temperature. Wells were then washed and

incubated with biotinylated polyclonal anti-gp120 antibody (20 μg/mL in DPBS) for two hours, and washed again with DPBS. The plate was then filled with DPBS while being stored at 4°C, ready for the virus capture step.

HIV-1 culture. We obtained HIV-1 samples from NIH under the AIDS Research and Reference Reagent Program. The viruses were cultured in peripheral blood mononuclear cells (PBMCs). PBMCs isolated from HIV-1 negative samples by Ficoll Hypaque density gradient centrifugation (Histopaque 1077 Sigma H8889) were stimulated with PHA (0.25 μg/mL) for 3 days and co-cultured with HIV-1 positive PBMCs samples. The samples were incubated at 37°C and 5% CO_2 atmosphere. P24 titer measurement was performed on the supernatants of the co-culture samples by an ELISA kit (Perkin Elmer®, NEK050b). When p24 titer in the samples reached 20 ng/mL, the co-culture was terminated. The viral load of the samples was quantified using Roche- COBAS® AmpliPrep/COBAS® TaqMan® HIV-1 Test, v2.0 system at the microbiology laboratory at the Brigham and Women's Hospital. The stock concentration of HIV-1 subtypes A, B, and D samples were 1.7×10^8, 1.2×10^8 and 2.9×10^8 copies/mL, respectively.

Virus capture. After antibody immobilization on PC nanostructures, HIV-1 samples were incubated in the modified wells for 30 minutes at room temperature in a BSL2+ cell culture facility. The wells were then washed three times with DPBS to remove any unbound viruses in the sample. Following washing, 4% of paraformaldehyde was added to fix the intact viruses for further analysis. The PWV shifts due to binding the viruses to the surface of the biosensor were measured for detection and quantification. For conducting the experiments in plasma, whole blood was centrifuged (1500 rpm) for 10 minutes to effectively separate the hematocrit. The plasma layer was gently collected. HIV-1 stocks (subtypes A and B) were thawed (from −80°C to room temperature) and diluted serially to achieve various virus concentrations in human plasma. Surface chemistry was performed on the PC surface, and the conjugated microwells were incubated with HIV-spiked plasma (100 μL), as well as a reference control of only plasma, for 1 hour at room temperature. After sample incubation, the microwells were carefully aspirated and 4%paraformaldehyde (100 μL) was added to fix the captured viruses. Post fixation, the wells were washed three times with DPBS and left wet with DPBS after the final wash. The PWV shifts were then measured.

HIV-1 sequencing. Viral RNA was extracted from 140 μL of cell culture supernatant using the QIAamp Viral RNA Mini Kit (Qiagen). The full-length envelope gene was amplified from RNA using a previously described nested PCR[68,69] modified with house-designed primers as previously described[70]. Bidirectional sequencing of near full-length HIV-1 envelope was performed using previously described primers[69]. Sequences were assembled using Sequencer software (GeneCodes). Ambiguous bases were called if individual chromatogram peak heights were at least 30% of the upper peak height. HIV-1 gp120 sequences were assembled to the EU541617 HIV-1 envelope sequence. This sequence was used to generate the polyclonal goat anti-gp120 antibody used in the experiments to capture and isolate HIV-1 subtypes.

Statistical analysis. The statistical analysis for the experimental results were performed using unpaired t test with 95% confidence internal and Analysis of Variance (ANOVA) with Tukey's post-hoc test and the statistical significance threshold was set at 0.05 (n = 3 to 6, p < 0.05).

1. Robinson, W. H. et al. Autoantigen microarrays for multiplex characterization of autoantibody responses. Nat. Med. 8, 295–301 (2002).
2. Wong, J., Sibani, S., Lokko, N. N., LaBaer, J. & Anderson, K. S. Rapid detection of antibodies in sera using multiplexed self-assembling bead arrays. J. Immunol. Methods 350, 171–182 (2009).
3. Ward, D. G. et al. Identification of serum biomarkers for colon cancer by proteomic analysis. Brit. J. Cancer 94, 1898–1905 (2006).
4. Nam, M. J. et al. Molecular profiling of the immune response in colon cancer using protein microarrays: Occurrence of autoantibodies to ubiquitin C-terminal hydrolase L3. Proteomics 3, 2108–2115 (2003).
5. Tannapfel, A. et al. Identification of novel proteins associated with hepatocellular carcinomas using protein microarrays. J. Pathol. 201, 238–249 (2003).
6. Patz, E. F. et al. Panel of serum biomarkers for the diagnosis of lung cancer. J. Clin. Oncol. 25, 5578–5583 (2007).
7. Zhang, Z. et al. Three biomarkers identified from serum proteomic analysis for the detection of early stage ovarian cancer. Cancer Res. 64, 5882–5890 (2004).
8. Luo, L. Y. et al. The serum concentration of human kallikrein 10 represents a novel biomarker for ovarian cancer diagnosis and prognosis. Cancer Res. 63, 807–811 (2003).
9. Diamandis, E. P. et al. Human kallikrein 6 (hK6): A new potential serum biomarker for diagnosis and prognosis of ovarian carcinoma. J. Clin. Oncol. 21, 1035–1043 (2003).
10. Diamandis, E. P. et al. Immunofluorometric quantification of human kallikrein 5 expression in ovarian cancer cytosols and its association with unfavorable patient prognosis. Tumor Biol. 24, 299–309 (2003).
11. Maurya, P., Meleady, P., Dowling, P. & Clynes, M. Proteomic approaches for serum biomarker discovery in cancer. Anticancer Res. 27, 1247–1255 (2007).
12. Salmanzadeh, A. et al. Isolation of prostate tumor initiating cells (TICs) through their dielectrophoretic signature. Lab Chip 12, 182–189 (2012).
13. Shafiee, H., Sano, M. B., Henslee, E. A., Caldwell, J. L. & Davalos, R. V. Selective isolation of live/dead cells using contactless dielectrophoresis (cDEP). Lab Chip 10, 438–445 (2010).
14. Klevan, L., Horton, L., Carlson, D. P. & Eisenberg, A. J. Chemiluminescent detection of DNA probes in forensic analysis. Electrophoresis 16, 1553–1558 (1995).
15. Wang, S., Xu, F. & Demirci, U. Advances in developing HIV-1 viral load assays for resource-limited settings. Biotechnol. Adv. 28, 770–781 (2010).
16. Wang, S. et al. Efficient on-chip isolation of HIV subtypes. Lab Chip 12, 1508–1515 (2012).
17. Shafiee, H. et al. Acute On-Chip HIV Detection Through Label-Free Electrical Sensing of Viral Nano-Lysate. Small 9, 2553–2563 (2013).
18. Inci, F. et al. Nanoplasmonic quantitative detection of intact viruses from unprocessed whole blood. ACS Nano 7, 4733–4745 (2013).
19. Lal, S., Link, S. & Halas, N. J. Nano-Optics from Sensing to Waveguiding. Nat. Photonics 1, 8 (2007).
20. Anker, J. N. et al. Biosensing with plasmonic nanosensors. Nat. Mater. 7, 442–453 (2008).
21. Arnold, S., Khoshsima, M., Teraoka, I., Holler, S. & Vollmer, F. Shift of whispering-gallery modes in microspheres by protein adsorption. Opt. Lett. 28, 272–274 (2003).
22. Fritz, J. et al. Translating biomolecular recognition into nanomechanics. Science 288, 316–318 (2000).
23. Tasoglu, S. et al. Manipulating biological agents and cells in micro-scale volumes for applications in medicine. Chem. Soc. Rev. 42, 5788–5808 (2013).
24. Cui, Y., Wei, Q., Park, H. & Lieber, C. M. Nanowire nanosensors for highly sensitive and selective detection of biological and chemical species. Science 293, 1289–1292 (2001).
25. Terrel, M., Digonnet, M. J. & Fan, S. Ring-coupled Mach-Zehnder interferometer optimized for sensing. Appl. Opt. 48, 4874–4879 (2009).
26. World Health Organization, Antiretroviral therapy in low- and middle-income countries by region. Available at: http://www.who.int/hiv/topics/treatment/data/en/ Accessed May 1 2013. (2011).
27. World Health Organization, HIV/AIDS, malaria and other diseases: HIV/AIDS indicators by country. Avilable at: http://apps.who.int/gho/data/node.main.559 Accessed May 10 2013. (2011).
28. Fiscus, S. A. et al. HIV-1 viral load assays for resource-limited settings. PLoS Med 3, e417 (2006).
29. World Health Organization, Guidelines for the Use of Antiretroviral Agents in HIV-1-Infected Adults and Adolescents, Available at: http://aidsinfo.nih.gov/contentfiles/lvguidelines/AdultandAdolescentGL.pdf. Accessed October 10 2013. (2013).
30. Mee, P., Fielding, K. L., Charalambous, S., Churchyard, G. J. & Grant, A. D. Evaluation of the WHO criteria for antiretroviral treatment failure among adults in South Africa. AIDS 22, 1971–1977 (2008).
31. van Oosterhout, J. J. G. et al. Diagnosis of antiretroviral therapy failure in Malawi: poor performance of clinical and immunological WHO criteria. Trop. Med. Int. Health 14, 856–861 (2009).
32. Vekemans, M., John, L. & Colebunders, R. When to switch for antiretroviral treatment failure in resource-limited settings? AIDS 21, 1205–1206 (2007).
33. Gale, H. B. et al. Is Frequent CD4+ T-Lymphocyte Count Monitoring Necessary for Persons With Counts ≥300 Cells/μL and HIV-1 Suppression? HIV/AIDS Brief Report 56, 4 (2013).
34. Schofield, D. J. & Dimmock, N. J. Determination of affinities of a panel of IgGs and Fabs for whole enveloped (influenza A) virions using surface plasmon resonance. J. Virol. Methods 62, 33–42 (1996).
35. Amano, Y. & Cheng, Q. Detection of influenza virus: traditional approaches and development of biosensors. Anal. Bioanal. Chem. 381, 156–164 (2005).
36. Boltovets, P. M. et al. Detection of plant viruses using a surface plasmon resonance via complexing with specific antibodies. J. Virol. Methods 121, 6 (2004).
37. Cooper, M. A. et al. Direct and sensitive detection of a human virus by rupture event scanning. Nat. Biotechnol. 19, 833–837 (2001).
38. Pineda, M. F., Chan, L. L., Kuhlenschmidt, T., Kuhlenschmidt, M. & Cunningham, B. T. rapid specific and label free detection of pocrine rotavirus using photonic crystal biosensors. IEEE Sensors 9, 8 (2009).
39. Patolsky, F. et al. Electrical detection of single viruses. Proc. Natl. Acad. Sci. U S A 101, 14017–14022 (2004).
40. Shamah, S. M. & Cunningham, B. T. Label-free cell-based assays using photonic crystal optical biosensors. Analyst 136, 12 (2011).
41. Chan, L. L., Gosangari, S. L., Watkin, K. L. & Cunningham, B. T. A label-free photonic crystal biosensor imaging method for detection of cancer cell cytotoxicity and proliferation. Apoptosis 12, 8 (2007).
42. Choi, C. J. & Cunningham, B. T. A 96-well microplate incorporating a replica molded microfluidic network integrated with photonic crystal biosensors for high throughput kinetic biomolecular interaction analysis. Lab Chip 7, 550–556 (2007).
43. Pineda, M. F. et al. Rapid Specific and Label-Free Detection of Porcine Rotavirus Using Photonic Crystal Biosensors. IEEE Sensors 9, 470–477 (2009).
44. Furin, J. J. et al. Expanding global HIV treatment: case studies from the field. Ann. N Y Acad. Sci. 1136, 12–20 (2008).
45. MH, M. The HIV-AIDS pandemic at 25 – the global response. N. Engl J. Med. 354, (2006).

46. Mamo, T. *et al.* Emerging nanotechnology approaches for HIV/AIDS treatment and prevention. *Nanomedicine (Lond)* **5**, 269–285 (2010).

47. Little, S. J., McLean, A. R., Spina, C. A., Richman, D. D. & Havlir, D. V. Viral dynamics of acute HIV-1 infection. *J. Exp. Med.* **190**, 841–850 (1999).

48. Rouet, F. *et al.* Transfer and evaluation of an automated, low-cost real-time reverse transcription-PCR test for diagnosis and monitoring of human immunodeficiency virus type 1 infection in a West African resource-limited setting. *J. Clin. Microbiol.* **43**, 2709–2717 (2005).

49. Rosenberg, N. E. *et al.* Point-of-care Diagnostics for Acute HIV Infection: An Important Public Health Priority. *J. Infect. Dis.* **206**, (2012).

50. Powers, K. A. *et al.* The role of acute and early HIV infection in the spread of HIV and implications for transmission prevention strategies in Lilongwe, Malawi: a modelling study. *Lancet* **378**, 256–268 (2011).

51. Koopman, J. S. *et al.* The role of early HIV infection in the spread of HIV through populations. *J. Acquir. Immune Defic. Syndr. Hum. Retrovirol.* **14**, 249–258 (1997).

52. Rosenberg, N. E. *et al.* Detection of acute HIV infection: a field evaluation of the determine(R) HIV-1/2 Ag/Ab combo test. *J. Infect. Dis.* **205**, 528–534 (2012).

53. Laperche, S., Leballais, L., Ly, T. D. & Plantier, J. C. Failure in the Detection of HIV p24 Antigen with the Determine HIV-1/2 Ag/Ab Combo Rapid Test. *J. Infect. Dis.* **206**, (2012).

54. Branson, B. & Stekler, J. Detection of Acute HIV Infection: We can't Close the Window. *J. Infect. Dis.* **205**, 4 (2011).

55. Busch, M. P. *et al.* Time course of detection of viral and serologic markers preceding human immunodeficiency virus type 1 seroconversion: implications for screening of blood and tissue donors. *Transfusion* **35**, 91–97 (1995).

56. Stroock, A. D. *et al.* Chaotic mixer for microchannels. *Science* **295**, 647–651 (2002).

57. Lee, W. G., Kim, Y. G., Chung, B. G., Demirci, U. & Khademhosseini, A. Nano/Microfluidics for diagnosis of infectious diseases in developing countries. *Adv. Drug Deliv. Rev.* **62**, 449–457 (2010).

58. Nowak, M. A. *et al.* Viral dynamics of primary viremia and antiretroviral therapy in simian immunodeficiency virus infection. *J. Virol.* **71**, 7518–7525 (1997).

59. World Health Organization, The use of Antiretroviral Drugs for Treatment and Preventing HIV Infection. Available at: http://apps.who.int/iris/bitstream/10665/85321/1/9789241505727_eng.pdf Accessed October 2013.

60. Stevens, W. S., Scott, L. E. & Crowe, S. M. Quantifying HIV for monitoring antiretroviral therapy in resource-poor settings. *J. Infect. Dis.* **201 Suppl 1**, S16–26 (2010).

61. Tanriverdi, S., Chen, L. & Chen, S. A rapid and automated sample-to-result HIV load test for near-patient application. *J. Infect. Dis.* **201 Suppl 1**, S52–58 (2010).

62. Usdin, M., Guillerm, M. & Calmy, A. Patient needs and point-of-care requirements for HIV load testing in resource-limited settings. *J. Infect. Dis.* **201 Suppl 1**, S73–77 (2010).

63. Kim, Y. G., Moon, S., Kuritzkes, D. R. & Demirci, U. Quantum dot-based HIV capture and imaging in a microfluidic channel. *Biosens. Bioelectron.* **25**, 253–258 (2009).

64. Wang, S., Inci, F., De Libero, G., Singhal, A. & Demirci, U. Point-of-care assays for tuberculosis: role of nanotechnology/microfluidics. *Biotechnol. Adv.* **31**, 438–449 (2013).

65. Wang, S. *et al.* Portable microfluidic chip for detection of Escherichia coli in produce and blood. *Int. J. Nanomed.* **7**, 2591–2600 (2012).

66. Moon, S. *et al.* Enumeration of CD4+ T-cells using a portable microchip count platform in Tanzanian HIV-infected patients. *PLoS ONE* **6**, e21409 (2011).

67. Cunningham, B. T. *et al.* Label-free assays on the BIND system. *J. Biomol. Screen.* **9**, 481–490 (2004).

68. Kirchherr, J. L. *et al.* High throughput functional analysis of HIV-1 env genes without cloning. *J. Virol. Methods* **143**, 104–111 (2007).

69. Sanders-Buell, E., Salminen, M. & McCutchan, F. Sequencing Primers for HIV-1. The Human Retroviruses and AIDS 1995 Compendium: The HIV Sequence Database and Analysis Project, Available at: http://www.hiv.lanl.gov/content/sequence/HIV/COMPENDIUM/1995/PART-III/3.pdf. Accessed October 30 2013, (1995).

70. Henrich, T. J. *et al.* Evolution of CCR5 antagonist resistance in an HIV-1 subtype C clinical isolate. *J. Acquir. Immune Defic. Syndr.* **55**, 420–427 (2010).

71. Wang, L. *et al.* Nanostructured substrates for isolation of circulating tumor cells. *Nano Today* **8**, 374–387 (2013).

Author contributions

H.S., B.C. and U.D. designed the study and the experiments, H.S., E.A.L. and M.J. performed the experiments and prepared Figures 2 and 3, H.S. prepared Figure 4, F.I. helped designing the surface chemistry for HIV-1 capture and prepared Figure 1, E.H. and T.J.H. sequenced the gp120 envelope of HIV-1 subtypes and prepared Figures S4-S6, D.R.K. supervised the virology aspect of the study and provided HIV subtype samples, H.S. and M.J. wrote the paper, B.C. and U.D. supervised the research.

Additional information

Supplementary information accompanies this paper at http://www.nature.com/scientificreports

Competing financial interests: Dr. Utkan Demirci is a founder of, and has an equity interest in, DxNow, a company that is developing microfluidic and imaging technologies for point-of-care diagnostic solutions. Dr. Utkan Demirci's interests were viewed and managed by the Brigham and Women's Hospital and Partners HealthCare in accordance with their conflict of interest policies.

How to cite this article: Shafiee, H. *et al.* Nanostructured Optical Photonic Crystal Biosensor for HIV Viral Load Measurement. *Sci. Rep.* **4**, 4116; DOI:10.1038/srep04116 (2014).